**JOURNAL OF THEORETICAL AND APPLIED MECHANICS**
**54**, 3, pp. 705-716, Warsaw 2016
DOI: 10.15632/jtam-pl.54.3.705

# COMBINED LOAD BUCKLING FOR CYLINDRICAL SHELLS BASED ON A SYMPLECTIC ELASTICITY APPROACH

Jiabin Sun
*State Key Laboratory of Structure Analysis for Industrial Equipment and School of Ocean Science and Technology, Dalian University of Technology, Panjin, P.R. China; e-mail: jbsun1983@dlut.edu.cn*

Xinsheng Xu
*State Key Laboratory of Structure Analysis of Industrial Equipment and Department for Engineering Mechanics, Dalian University of Technology, Dalian, P.R. China*

C.W. Lim
*Department of Civil and Architectural Engineering, City University of Hong Kong, Hong Kong, P.R. China*

Buckling behavior of cylindrical shells subjected to combined pressure, torsion and axial compression is presented by employing a symplectic method. Both symmetric and non-symmetric boundary conditions are considered. Hamiltonian canonical equations are established by introducing four pairs of dual variables. Then, solution of fundamental equations is converted into a symplectic eigenvalue problem. It is concluded that the influence of pressure on buckling solutions is more significant than that due to compressive load, in particular for a longer external pressured cylindrical shell. Besides, buckling loads and circumferential wavenumbers can be reduced greatly by relaxed in-plane axial constraints.

*Keywords:* buckling mode, combined loads, critical load, cylindrical shell, symplectic method

## 1. Introduction

In practical applications, thin-walled cylindrical shells are not usually subject to only one single loading condition but very commonly they are subject to a combination of three basic types of loads, i.e. torsional load, pressure and axial compressive load. Therefore, it is very meaningful to understand the interactive buckling behavior of cylindrical shells under the combined action of two or all of these loads. In the previous theoretical studies, various approximate methods were developed to predict the buckling loads of cylindrical shells with special boundary conditions. One common numerical approximation is to assume a suitable series expansion for the displacement, and subsequently transform the basic problem into a system of linear equations like in the Galerkin method. Kardomateas and Philobos (1996) presented benchmark solutions for instability of a thick-walled cylindrical shell under combined axial compression and external pressure by separating variables and transforming higher-order partial differential equations into ordinary differential equations. Despite obtaining more accurate results, it is necessary to assume some forms of admissible displacement expressions. The solution space is also incomplete. Another feasible approximate approach is to apply perturbation techniques to deal with the buckling of shells with more complex physical properties. Some other approaches include analytical studies by Anastasiadis *et al.* (1994) and Shen and Xiang (2008). In addition to the analytical and perturbation methods, the rapidly developing computational hardware and software also offer great opportunities to challenge the complex buckling problems. For example, Mao and Lu (2001) used the finite difference method to study plastic buckling of a thin-walled cylindrical shell subjected to combined action of general loads based on the $J_2$ deformation theory. Tafreshi (2006) and

Vaziri and Estekanchi (2006) investigated buckling and post-buckling cylindrical shells subjected to pressure and axial compression by means of the finite-element method. By employing the semi-analytical finite-element method, Ley *et al.* (1994) studied buckling loads of ring-stiffened anisotropic cylinders subjected to axial compression, torsion, and internal pressure.

Most of the solution methods cited above can be regarded as approximate or numerical methods, and most of the studies considered only two loads. It is very rare that three types of loads are considered. The classical analytical methods which apply a Lagrangian system involve only one type of variables. In the systems, the basic equations are expressed in higher-order partial differential equations and even after separating the variables, analytical solutions are rather difficult to be derived. In view of these shortcomings, Zhong (2004) presented a symplectic analytical theory to establish a standardized solution procedure for some fundamental problems in solid mechanics. Applying the Legendre transformation, higher-order Lagrange governing equations can be converted to lower-order Hamiltonian dual equations. Hence, analytical solutions can be subsequently obtained by separating variables in the symplectic space. This symplectic analytical method is not only rigorous, but it also establishes a rational solution procedure. In this regard, Xu *et al.* (2006) investigated local buckling and axial stress waves propagation (and reflection). They developed a Hamiltonian system for solving dynamic buckling of cylindrical shells. Recently, based on classical Donnell's shell theory, the authors (2014) presented a symplectic solving method for buckling of cylindrical shells under pressure.

The main objective of this paper is the bifurcation buckling of cylindrical shells subjected to a combination of pressure, torsion and compressive loads. Various combinations of in-plane and transverse boundary conditions at both shell edges are considered. Applying the symplectic approach, the Hamiltonian governing equations are obtained through the Hamiltonian principle of mixed energy. Then the buckling loads and buckling modes can be related to the symplectic eigenvalues and eigenvectors, respectively. The parameters which influence the shell buckling are analyzed and discussed using some numerical examples.

## 2. Fundamental problem and Hamiltonian system

A cylindrical shell with radius $R$, length $l$, thickness $t$, Young's modulus $E$ and Poisson's ratio $\nu$, as shown in Fig. 1, which is acted by a combination of loads including pressure $P$ (positive for an external pressure), torque $T$ and compressive load $N$ is considered. A circular cylindrical coordinate with the $x$-axis along the shell axis is adopted, and $u$, $v$, $w$ denote the corresponding displacements along with the $x$-direction, $\theta$-direction and $r$-direction, respectively.

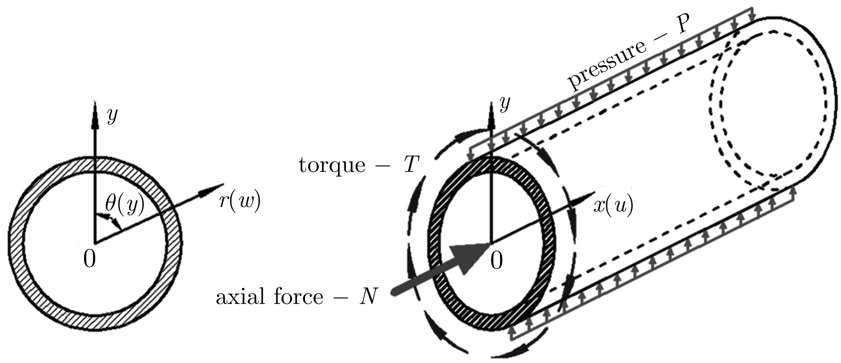


Fig. 1. Geometric parameters of a cylindrical shell subjected to combined loads

The constitutive relations are expressed as (Yamaki, 1984)

$$
\begin{aligned}
N_x &= K\Big[\frac{\partial u}{\partial x}+\frac{\nu}{R}\Big(\frac{\partial v}{\partial \theta}-w\Big)\Big] & M_x &= -D\Big(\frac{\partial^2 w}{\partial x^2}+\frac{\nu}{R^2}\frac{\partial^2 w}{\partial \theta^2}\Big)\\
N_\theta &= K\Big[\frac{1}{R}\Big(\frac{\partial v}{\partial \theta}-w\Big)+\nu\frac{\partial u}{\partial x}\Big] & M_\theta &= -D\Big(\frac{1}{R^2}\frac{\partial^2 w}{\partial \theta^2}+\nu\frac{\partial^2 w}{\partial x^2}\Big)\\
N_{x\theta} &= \frac{K(1-\nu)}{2}\Big(\frac{1}{R}\frac{\partial u}{\partial \theta}+\frac{\partial v}{\partial x}\Big) & M_{x\theta} &= -\frac{D(1-\nu)}{R}\frac{\partial^2 w}{\partial x\partial \theta}
\end{aligned}
\tag{2.1}
$$

where $D = Et^3/[12(1-\nu 2)]$ and $K = Et/(1-\nu^2)$. Introducing a stress function $\phi$, the membrane forces can be expressed as

$$
N_x = \frac{1}{R^2}\frac{\partial^2 \phi}{\partial \theta^2} \qquad N_\theta = \frac{\partial^2 \phi}{\partial x^2} \qquad N_{x\theta} = -\frac{1}{R}\frac{\partial^2 \phi}{\partial x \partial \theta}
\tag{2.2}
$$

Based on Donnell's shell theory and neglecting the pre-buckling bending effect, the internal forces of the buckling state can be obtained as $N_x^0 = N/(2\pi R)$, $N_\theta^0 = -pR$ and $N_{x\theta}^0 = T/(2\pi R)$. From the variational principle, the Lagrange density function can be expressed in terms of elastic potential energy and work due to the external load, as

$$
\begin{aligned}
\overline{L} = {}& \frac{1}{R^2}\frac{\partial^2 \phi}{\partial \theta^2}\frac{\partial u}{\partial x}+\frac{\partial^2 \phi}{\partial x^2}\Big(\frac{1}{R}\frac{\partial v}{\partial \theta}-\frac{w}{R}\Big)-\frac{1}{R}\frac{\partial^2 \phi}{\partial x\partial \theta}\Big(\frac{1}{R}\frac{\partial u}{\partial \theta}+\frac{\partial v}{\partial x}\Big)-\frac{1}{2Eh}\Big(\frac{\partial^2 \phi}{\partial x^2}+\frac{1}{R^2}\frac{\partial^2 \phi}{\partial \theta^2}\Big)^2\\
&+\frac{D}{2}\Big(\frac{\partial^2 w}{\partial x^2}+\frac{1}{R^2}\frac{\partial^2 w}{\partial \theta^2}\Big)^2-\frac{N_x^0}{2}\Big(\frac{\partial w}{\partial x}\Big)^2-\frac{T_{x\theta}^0}{R}\frac{\partial w}{\partial x}\frac{\partial w}{\partial \theta}-\frac{N_\theta^0}{2R^2}\Big(\frac{\partial w}{\partial \theta}\Big)^2
\end{aligned}
\tag{2.3}
$$

According to the variational equation $\delta\iint \overline{L}\; dS = 0$, the compatibility condition and equilibrium equation can be obtained in the Lagrange system. For simplicity, the following dimensionless terms are defined as $X = x/R$, $U = u/R$, $V = v/R$, $W = w/R$, $\varPhi = \phi/(Et^3)$, $L = l/R$, $H = t/R$, $\alpha = 12(1-\nu^2)$, $\beta = \alpha H^2$, $N_{cr} = N_x^0 R^2/D$, $T_{cr} = T_{x\theta}^0 R^2/D$ and $P_{cr} = N_\theta^0/D$. An over-dot denotes differentiation with respect to $\theta$, i.e. $\dot{W} = \partial W/\partial\theta$, in which the $\theta$-coordinate is taken as a time-equivalent coordinate and $\partial_X W = \partial W/\partial X$. Introducing two additional variables, $\xi = -\dot{W}$ and $\varphi = -\dot{\varPhi}$, the dimensionless Lagrange density function can be expressed as

$$
L = -\alpha W\partial_X^2\varPhi-\frac{\beta}{2}(\partial_X^2\varPhi+\ddot{\varPhi})^2+\frac{1}{2}(\partial_X^2 W+\ddot{W})^2-\frac{N_{cr}}{2}(\partial_X W)^2-T_{cr}\dot{W}\partial_X W-\frac{P_{cr}}{2}(\dot{W})^2
\tag{2.4}
$$

Applying Legendre's transformation, a vector $\mathbf{q} = [W,\xi,\varPhi,\varphi]^{\mathrm{T}}$ is introduced and the corresponding dual vector, defined as $\mathbf{p} = [p_1,p_2,p_3,p_4]^{\mathrm{T}}$, can be derived from $\mathbf{p} = \delta L/\delta\dot{\mathbf{q}}$. The elements of $\mathbf{p} = [p_1,p_2,p_3,p_4]^{\mathrm{T}}$ represent the equivalent transverse shear force, bending moment, shear stress and normal stress, in the Hamiltonian system, respectively. Then, the Hamiltonian density function is given by $H(\mathbf{q},\mathbf{p}) = \mathbf{p}^{\mathrm{T}}\dot{\mathbf{q}} - L(\mathbf{q},\mathbf{p})$ and the Hamiltonian canonical equations are

$$
\begin{Bmatrix}\dot{\mathbf{q}}\\ \dot{\mathbf{p}}\end{Bmatrix} = \begin{Bmatrix}\dfrac{\delta H}{\delta \mathbf{p}}\\ -\dfrac{\delta H}{\delta \mathbf{q}}\end{Bmatrix} = \begin{bmatrix}\mathbf{A} & \mathbf{B}\\ \mathbf{C} & -\mathbf{A}^{\mathrm{T}}\end{bmatrix}\begin{Bmatrix}\mathbf{q}\\ \mathbf{p}\end{Bmatrix}
\tag{2.5}
$$

where

$$\mathbf{A} = \begin{bmatrix} 0 & -1 & 0 & 0 \\ \partial_X^2 & 0 & 0 & 0 \\ 0 & 0 & 0 & -1 \\ 0 & 0 & \partial_X^2 & 0 \end{bmatrix} \qquad \mathbf{B} = \begin{bmatrix} 0 & 0 & 0 & 0 \\ 0 & 1 & 0 & 0 \\ 0 & 0 & 0 & 0 \\ 0 & 0 & 0 & -\dfrac{1}{\beta} \end{bmatrix}$$

$$\mathbf{C} = \begin{bmatrix} N_{cr}\partial_X^2 & -T_{cr}\partial_X & -\alpha\partial_X^2 & 0 \\ T_{cr}\partial_X & -P_{cr} & 0 & 0 \\ -\alpha\partial_X^2 & 0 & 0 & 0 \\ 0 & 0 & 0 & 0 \end{bmatrix}$$

Defining a state vector $\boldsymbol{\psi} = [\mathbf{q}^{\mathrm{T}}, \mathbf{p}^{\mathrm{T}}]^{\mathrm{T}}$, Eq. (2.5) can be simplified as

$$\dot{\boldsymbol{\psi}} = \mathbf{H}\boldsymbol{\psi} \tag{2.6}$$

where $\mathbf{H}$ is the Hamiltonian operator matrix (Zhong, 2004).

## 3. Symplectic eigenvalue problem

In a symplectic system, the solution to Eq. (2.6) can be derived by separating the variables, i.e. $\boldsymbol{\psi}(X,\theta) = \boldsymbol{\eta}(X)\chi(\theta)$. Hence, Eq. (2.6) can be simplified to

$$\chi(\theta) = \mathrm{e}^{\mu\theta} \qquad \mathbf{H}\boldsymbol{\eta}(X) = \mu\boldsymbol{\eta}(X) \tag{3.1}$$

where $\boldsymbol{\eta} = [q_1', q_2', q_3', q_4', p_1', p_2', p_3', p_4']$ and $\mu$ represent the symplectic eigenvector and eigenvalue, respectively. For a shell of revolution, the continuity condition requires $\boldsymbol{\psi}(X,0) = \boldsymbol{\psi}(X,2\pi)$ and the eigenvalues are $\mu_n = n\mathrm{i}$ $(n = 0, \pm 1, \pm 2, \ldots)$. Substituting it into Eq. (3.1), the symplectic eigenvalue equation can be expressed as

$$\mathbf{H}\boldsymbol{\eta}_n = n\mathrm{i}\boldsymbol{\eta}_n \tag{3.2}$$

The characteristic polynomial of Eq. (3.2) is

$$\lambda^8 + a\lambda^6 + b\lambda^5 + c\lambda^4 + d\lambda^3 + e\lambda^2 + f\lambda + g = 0 \tag{3.3}$$

where $a = -4n^2 + N_{cr}$, $b = 2nT_{cr}\mathrm{i}$, $c = 6n^4 - 2n^2N_{cr} - n^2P_{cr} + \alpha^2/\beta$, $d = -4n^3T_{cr}\mathrm{i}$, $e = -4n^6 + n^4N_{cr} + 2n^4P_{cr}$, $f = 2n^5T_{cr}\mathrm{i}$ and $g = n^8 - n^6P_{cr}$. Solving Eq. (3.3) in the complex domain, the $n$-th order eigenvector of Eq. (3.2) is given by

$$\boldsymbol{\eta}_n = \sum_{k=1}^{8} \mathbf{c}_k \mathrm{e}^{\lambda_k X} \tag{3.4}$$

where $\mathbf{c}_k = [c_{1k}, c_{2k}, \ldots, c_{8k}]^{\mathrm{T}}$ $(k = 1, 2, \ldots, 8)$ is a vector which consists of eight unknown constants which can be determined from the boundary conditions. The eight characteristic roots of Eq. (3.3) are $\lambda_k$ $(k = 1, 2, \ldots, 8)$. Thus, the buckling solution can be expanded as

$$\boldsymbol{\psi}(X,\theta) = \sum_{n=1}^{\infty}\sum_{k=1}^{8}\Big(a_n\mathbf{c}_k^{(n)}\mathrm{e}^{\lambda_k(n)X}\mathrm{e}^{n\theta\mathrm{i}} + b_n\mathbf{c}_k^{(-n)}\mathrm{e}^{\lambda_k(-n)X}\mathrm{e}^{-n\theta\mathrm{i}}\Big) \tag{3.5}$$

where $a_n$ and $b_n$ are the undetermined coefficients, and each expansion term of Eq. (3.5) is a buckling mode.

## 4. Boundary conditions and buckling bifurcation condition

In a Lagrangian system, the transverse boundary conditions are generally expressed in terms of displacement components and internal forces. In a Hamiltonian system, the conditions must be expressed in terms of the Hamilton dual variables. The clamped boundary conditions are

$$W = q_1\Big|_{X=\pm L/2} = 0 \qquad \partial_X W = \partial_X q_1\Big|_{X=\pm L/2} = 0 \tag{4.1}$$

and the simply supported boundary conditions are

$$W = q_1\Big|_{X=\pm L/2} = 0 \qquad \partial_X^2 W = \partial_X^2 q_1\Big|_{X=\pm L/2} = 0 \tag{4.2}$$

In addition to transverse constraints, the in-plane boundary conditions are also necessary. From Eq. (3.1), the displacement conditions $U = 0$ and $V = 0$ can be expressed in equivalent forms as $\partial_\theta^2 U = 0$ and $\partial_\theta V = 0$ (Yamaki, 1984). Hence, the in-plane boundary conditions are:

— Case 1

$$\begin{aligned} \partial_\theta^2 U &= \Big(-(1+\nu)\partial_X^3 q_3 + \frac{2+\nu}{\beta}\partial_X p_4 + \frac{1}{H^2}\partial_X q_1\Big)\Big|_{X=\pm L/2} = 0 \\ \partial_\theta V &= \Big((1+\nu)\partial_X^2 q_3 - \frac{\nu p_4}{\beta} + \frac{q_1}{H^2}\Big)\Big|_{X=\pm L/2} = 0 \end{aligned} \tag{4.3}$$

— Case 2

$$\begin{aligned} \partial_\theta^2 U &= \Big((1+\nu)\partial_X^3 q_3 - \frac{\nu}{\beta}\partial_X p_4 + \frac{1}{H^2}\partial_X q_1\Big)\Big|_{X=\pm L/2} = 0 \\ N_{X\theta} &= \partial_X q_4\Big|_{X=\pm L/2} = 0 \end{aligned} \tag{4.4}$$

— Case 3

$$\begin{aligned} N_X &= \Big(\frac{p_4}{\beta} - \partial_X^2 q_3\Big)\Big|_{X=\pm L/2} = 0 \\ \partial_\theta V &= \Big(\partial_X^2 q_3 + \frac{q_1}{H^2}\Big)\Big|_{X=\pm L/2} = 0 \end{aligned} \tag{4.5}$$

— Case 4

$$\begin{aligned} N_X &= \Big(\frac{p_4}{\beta} - \partial_X^2 q_3\Big)\Big|_{X=\pm L/2} = 0 \\ N_{X\theta} &= \partial_X q_4\Big|_{X=\pm L/2} = 0 \end{aligned} \tag{4.6}$$

By using Eq. (3.4) and some specified boundary conditions, a homogeneous system consisting of eight linear equations can be obtained as

$$\mathbf{D}\mathbf{c}_1 = \mathbf{0} \tag{4.7}$$

where $\mathbf{c}_1 = [c_{11}, c_{12}, \ldots, c_{18}]^{\mathrm{T}}$ is the undetermined coefficients vector, and $D_{ij}(T_{cr}, N_{cr}, P_{cr}, n)$ are elements of the matrix $\mathbf{D}$ which is related to combinations of boundary cases, see Eqs. (4.1)-(4.6). For the non-trivial solution, the determinant of $\mathbf{D}$ must vanish, or

$$|\mathbf{D}|_{8\times 8} = 0 \tag{4.8}$$

Consequently, the relationship of critical loads $(T_{cr}, N_{cr}, P_{cr})$ and buckling mode can be determined from Eq. (4.8) and Eq. (3.4).

## 5. Buckling results and discussion

Here, for convenience, a curvature parameter $Z = \sqrt{1-\nu^2}L^2/H$ is adopted. In the numerical examples, the cylindrical shells have dimensionless thickness $H = t/R = 0.01$ and Poisson's ratio $\nu = 0.3$. Various combinations of transverse and in-plane boundary conditions are assumed. For two specified loads (either two of pressure $P_{cr}$, torque $T_{cr}$ or axial load $N_{cr}$), the critical value for the remaining load can always be determined from bifurcation condition, Eq. (4.8). As an example, for some specified pressure and compressive load which act on the shell, the torsional buckling load can be obtained.

From Eq. (3.1), integer $n$ denotes the number of buckling waves in the circumferential direction while the corresponding buckling mode can be referred as the $n$-th order mode. As mentioned above, torsional buckling loads for various boundary conditions are illustrated in Figs. 2 and 3 for $Z = 500$. In general, it is observed that the effect of pressure is more significant than that due to axial compression. The buckling load goes up with increasing internal pressure but decreases with growing external pressure. This observation is consistent with other published results (Yamaki, 1984; Winterstetter and Schmidt, 2002). The result indicates that a cylindrical shell loses stability more easily when acted by an external pressure. For in-plane boundary conditions, it is noted that relaxing the in-plane axial constraint greatly reduces the buckling torsional load. Comparatively, the transverse boundary conditions do have relatively limited effect on buckling solutions. In Figs. 4 and 5, the buckling modes corresponding to various boundary conditions are presented for $P_{cr} = 20$ and $N_{cr} = 200$. It also clearly shows that the in-plane boundary conditions play an important role on the relevant buckling behavior.

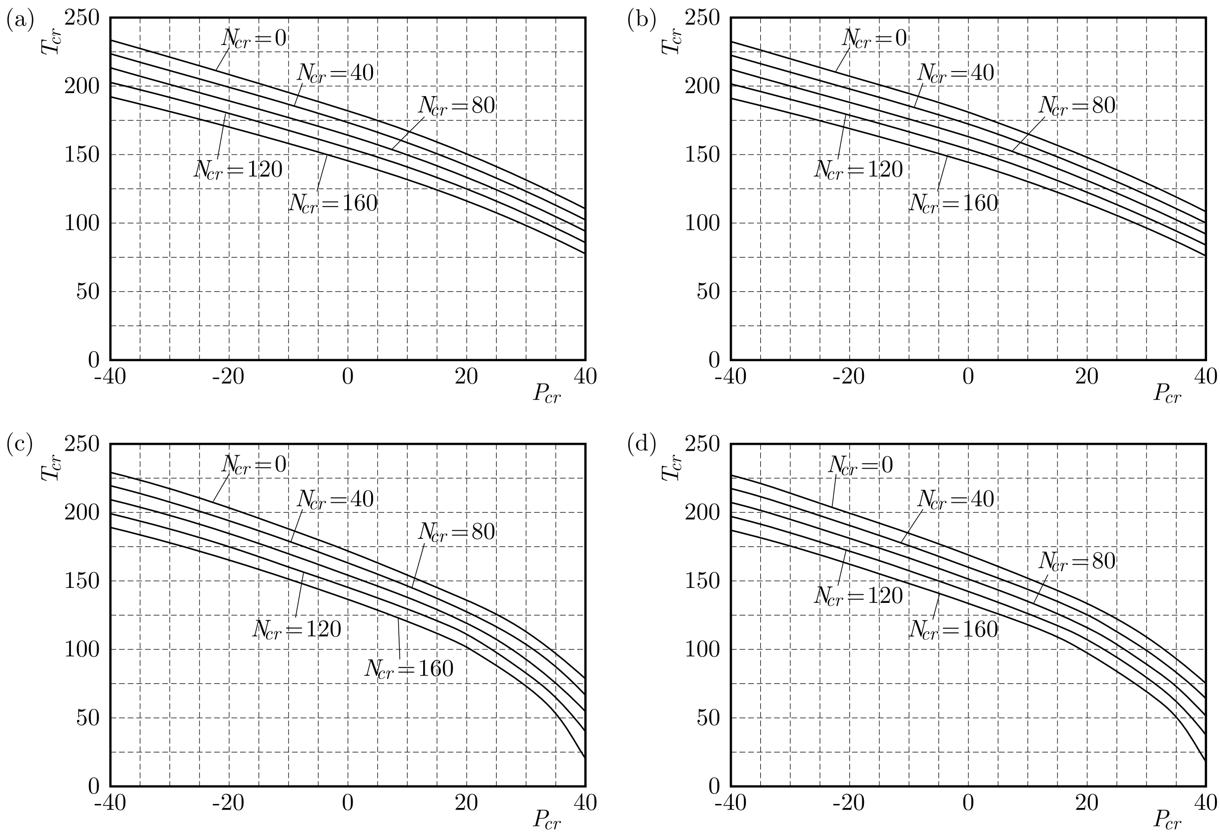


Fig. 2. $T_{cr}$ vs. $P_{cr}$ under clamped boundary conditions: (a) Case 1, (b) Case 2, (c) Case 3, (d) Case 4

Here, a case with clamped transverse constraints in Eq. (4.2) and Case 1 with in-plane constraints in Eq. (4.4) is considered. The buckling loads with the increasing shell length are

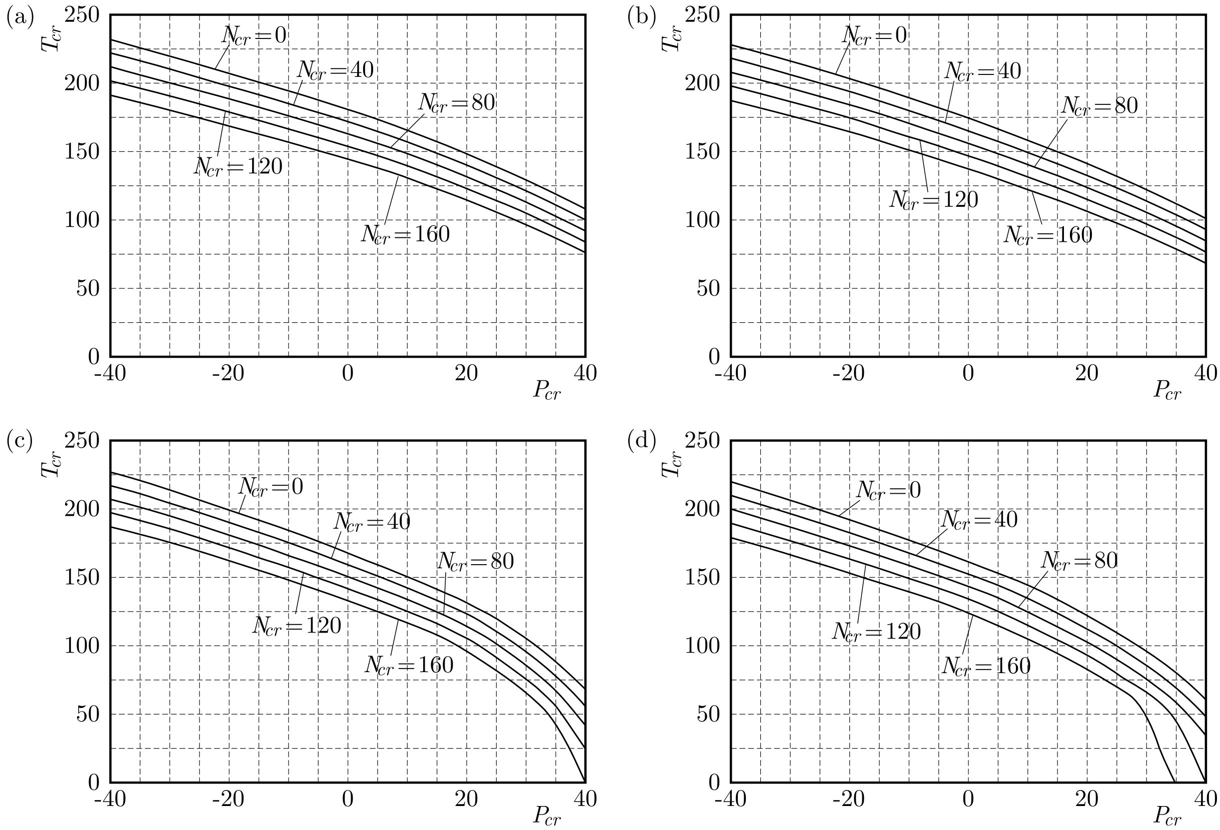


Fig. 3. $T_{cr}$ vs. $P_{cr}$ under simply supported boundary conditions: (a) Case 1, (b) Case 2, (c) Case 3, (d) Case 4

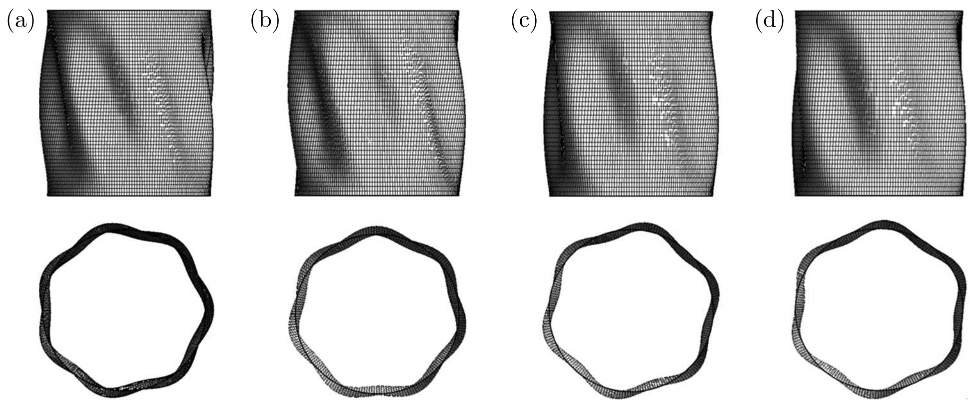


Fig. 4. Buckling modes for clamped boundary conditions: (a) Case 1, (b) Case 2, (c) Case 3, (d) Case 4

illustrated in Fig. 6. It is noticed that the buckling loads rapidly decrease with an increase in the shell length. The corresponding buckling modes for $P_{cr} = 20$ and $N_{cr} = 200$ are shown in Fig. 7. The axial waveforms which vary with $Z$ are also observed in the figure. For a fixed axial compressive load ($N_{cr} = 200$) and curvature parameter ($Z = 1000$), the effect of buckling modes with respect to the external and internal pressure is shown in Fig. 8. It is clearly observed that the shell is twisted intensively with the increasing internal pressure. However, this effect reverses completely if the shell is acted by an external pressure. The effect of compressive load on the buckling modes is presented in Fig. 9 for $P_{cr} = 40$. It shows that an increase in the axial load have a insignificant influence on the buckling deformation.

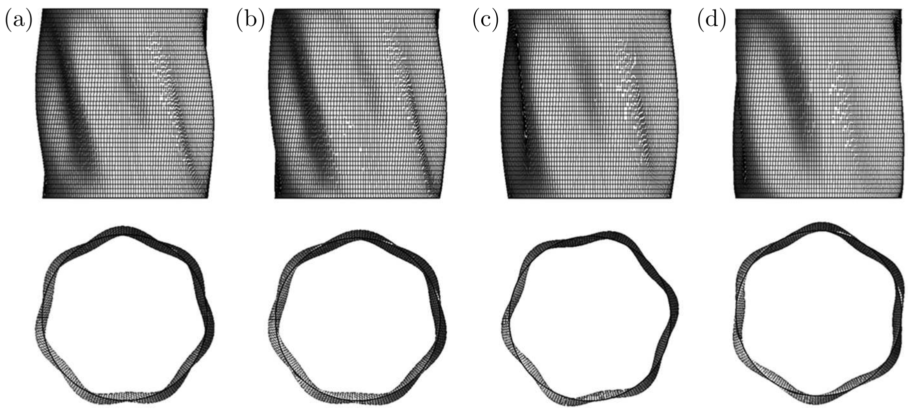


Fig. 5. Buckling modes for simply supported boundary conditions: (a) Case 1, (b) Case 2, (c) Case 3, (d) Case 4

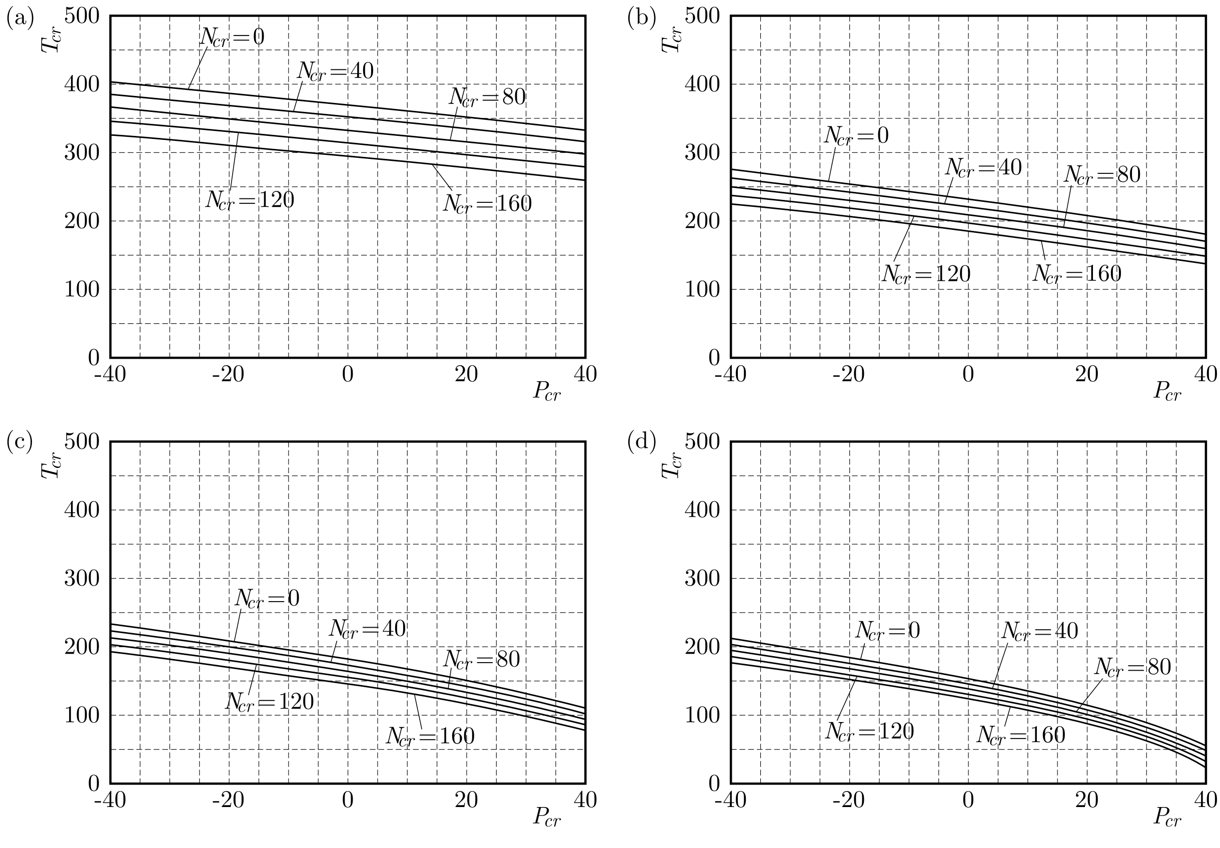


Fig. 6. $T_{cr}$ vs. $P_{cr}$ under different curvature parameters $Z$: (a) $Z = 50$, (b) $Z = 200$, (c) $Z = 500$, (d) $Z = 1000$

To study the effect of thickness on the buckling behavior, shells of thickness 0.002 and 0.005 are considered additionally. The buckling solutions for the shell with $L = 2$ are illustrated in Fig. 10. The critical load is redefined as $\overline{T}_{cr} = H^2 T_{cr}$. In the figure, it is observed that the buckling torsional load increases for a thicker shell. For similar loading conditions, the corresponding axial buckling modes are presented in Fig. 11. The figure indicates that the buckling waves become densely for a thinner shell.

Next, the buckling response of cylindrical shells subjected to non-symmetric boundary conditions is investigated. In this example, the shell has clamped transverse constraints and Case 1 in-plane constraints at $X = 0$. At the other end, the simply supported plus Case 1

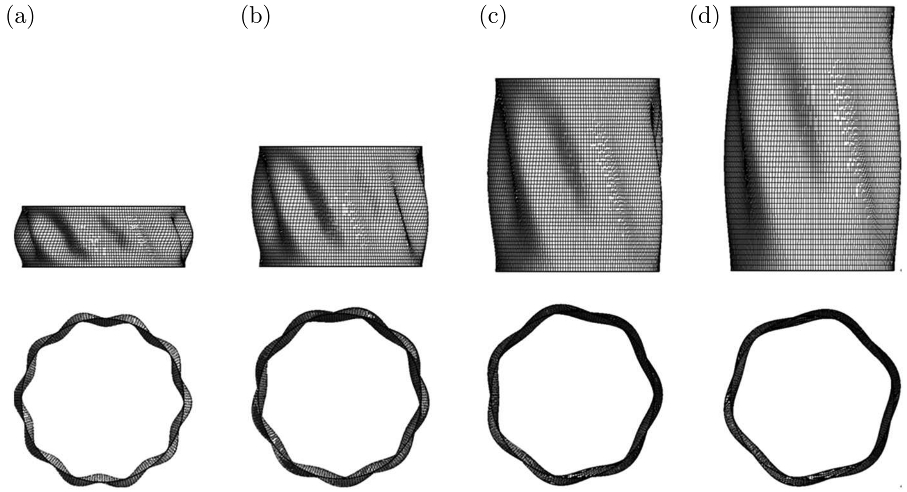


Fig. 7. Buckling mode with different curvature parameters $Z$: (a) $Z = 50$, (b) $Z = 200$, (c) $Z = 500$, (d) $Z = 1000$

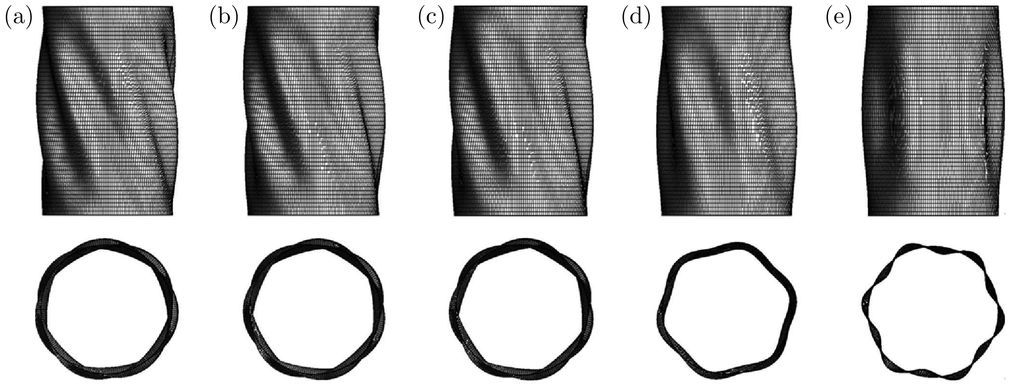


Fig. 8. Buckling modes under different pressure $P_{cr}$: (a) $P_{cr} = -40$, (b) $P_{cr} = -20$, (c) $P_{cr} = 0$, (d) $P_{cr} = 20$, (e) $P_{cr} = 40$

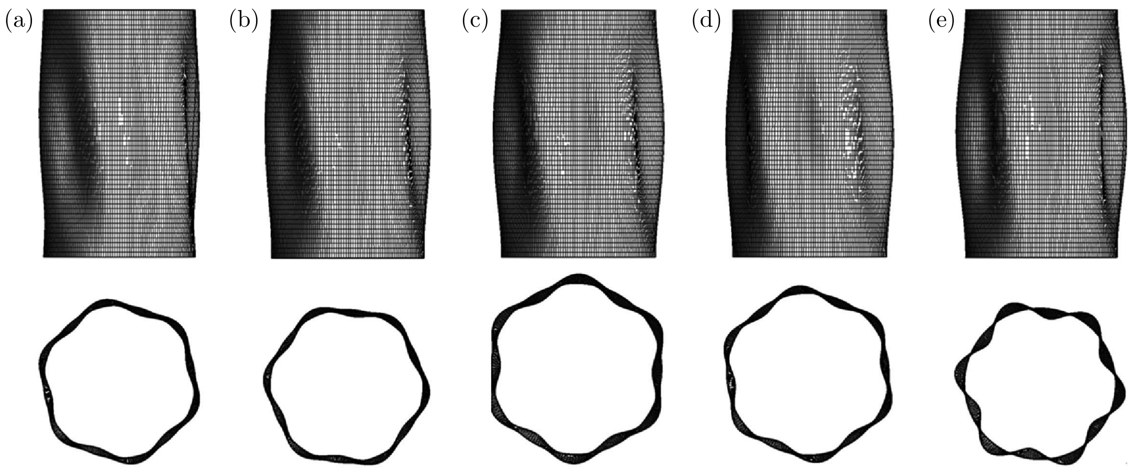


Fig. 9. Buckling modes under different compressive load $N_{cr}$: (a) $N_{cr} = 0$, (b) $N_{cr} = 40$, (c) $N_{cr} = 80$, (d) $N_{cr} = 120$, (e) $N_{cr} = 160$

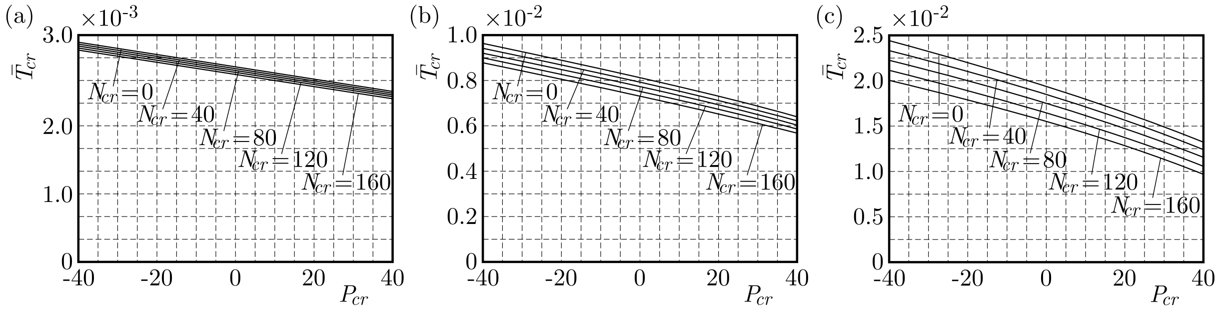


Fig. 10. $\overline{T}_{cr}$ vs. $P_{cr}$: (a) $H = 0.002$, (b) $H = 0.005$, (c) $H = 0.01$

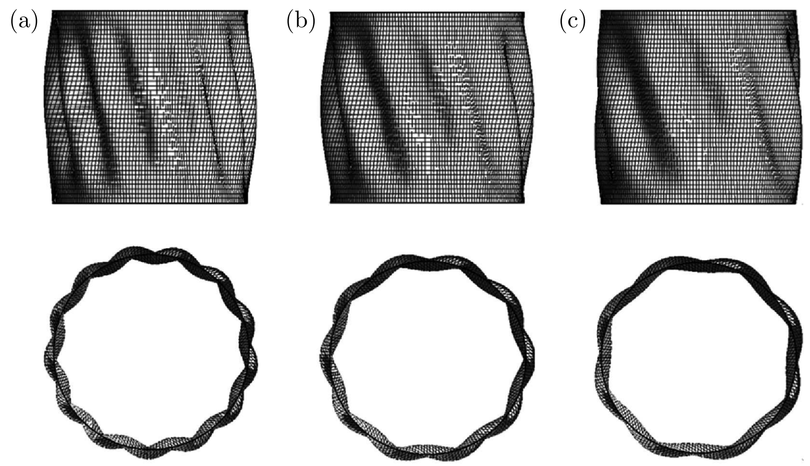


Fig. 11. Buckling modes for different shell thicknesses $H$: (a) $H = 0.002$, (b) $H = 0.005$, (c) $H = 0.01$

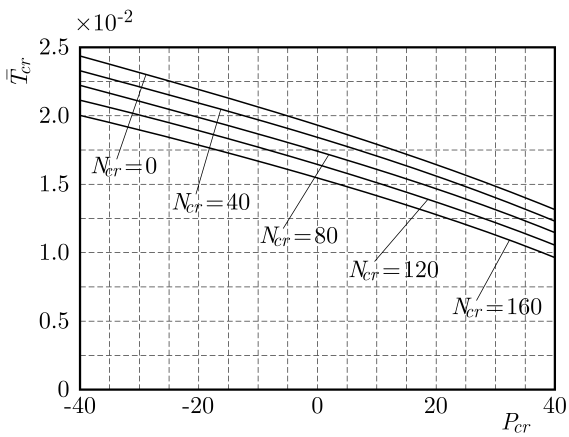


Fig. 12. $T_{cr}$ vs. $P_{cr}$ for the non-symmetric boundary condition (clamped at one end and simply supported at the other end)

constraints are applied. The buckling loads and buckling modes are presented in Figs. 12. The curvature parameter $Z = 500$ and thickness $H = 0.01$ are selected. Compared with Figs. 2a and 3a, it can be found that the obtained torsional loads are smaller than those of the symmetric clamped shells and larger than those of the symmetric simply supported shells.

## 6. Conclusion

A very effective Hamiltonian system constructed within a symplectic space for buckling of cylindrical shells subjected to a combination of pressure, torsion and axial compression is established. Applying Legendre's transformation, the Hamiltonian canonical equations are derived by introducing four pairs of dual variables. By separating the variables, the classical governing equation is converted to a symplectic eigenvalue problem where only solutions for the symplectic eigenvalues and eigenvectors are required.

Through a systematic and rational procedure, it is derived that the eigensolutions for the zero-eigenvalues and non-zero-eigenvalues represent axisymmetric and non-axisymmetric shell buckling modes, respectively. For cylindrical shells subjected to pressure and axial compression, the numerical examples concluded that: (i) buckling torsional loads should go up with an increase in the internal pressure and decline with a rise in the external pressure and compressive load. These changings induced by the applied pressure become more significant. For buckling modes, the effect of pressure load on the twisted waveforms is also more obvious that caused by axial compression; (ii) with the relaxation of the in-plane axial constraint, the downtrend of buckling loads with respect to pressure should be more dramatic. And the corresponding buckling mode also presents a slight twisted shape. Besides, the transverse boundary conditions have a limited influence on buckling results while external pressures are not extremely large; (iii) buckling torsional loads should be reduced for longer and thinner shells. The circumferential waves number of the buckling mode increases with a decrease in the thickness and length of the shell; (iv) for shells with non-symmetric boundary constrains, the buckling solutions fall in between those under the corresponding symmetric boundary conditions.

*Acknowledgements*

The supports of National Natural Science Foundation of China (No. 11402050), the Fundamental Research Funds for the Central Universities (No. DUT15LK46) and the Natural Science Foundation of China (No. 11372070) are acknowledged.

## References

1. Anastasiadis J.S., Tabiei A., Simitses G.J., 1994, Instability of moderately thick, laminated cylindrical shells under combined axial compression and pressure, *Composite Structures*, **27**, 4, 367-378
2. Kardomateas G.A., Philobos M.S., 1995, Buckling of thick orthotropic cylindrical shells under combined external pressure and axial compression, *AIAA Journal*, **33**, 10, 1946-1953
3. Ley R.P., Johnson E.R., Guerdal Z., 1994, Buckling of imperfect, anisotropic, ring-stiffened cylinders under combined loads, *AIAA Journal*, **32**, 6, 1302-1309
4. Mao R.J., Lu G., 2001, Plastic buckling of circular cylindrical shells under combined in-plane loads, *International Journal of Solids and Structures*, **38**, 741-757
5. Shen H.S., Xiang Y., 2008, Buckling and postbuckling of anisotropic laminated cylindrical shells under combined axial compression and torsion, *Composite Structures*, **84**, 375-386
6. Sun J.B., Xu X.S., Lim C.W., 2014, Buckling of cylindrical shells under external pressure in a Hamiltonian system, *Journal of Theoretical and Applied Mechanics*, **52**, 3, 641-653
7. Tafreshi A., 2006, Delamination buckling and postbuckling in composite cylindrical shells under combined axial compression and external pressure, *Composite Structures*, **72**, 401-418
8. Vaziri A., Estekanchi H.E., 2006, Buckling of cracked cylindrical thin shells under combined internal pressure and axial compression, *Thin-Walled Structures*, **44**, 141-151

9. Winterstetter T.A., Schmidt H., 2002, Stability of circular cylindrical steel shells under combined loading, *Thin-Walled Structures*, **40**, 893-909

10. Xu X.S., Ma Y., Lim C.W., Chu H.J., 2006, Dynamic buckling of cylindrical shells subject to an axial impact in a symplectic system, *International Journal of Solids and Structures*, **43**, 3905-3919

11. Yamaki N., 1984, *Elastic Stability of Circular Cylindrical Shells*, North Holland, Amsterdam/New York/Oxford

12. Zhong W.X., 2004, *Duality System in Applied Mechanics and Optimal Control*, Kluwer Academic Publishers, Boston


*Manuscript received May 7, 2015; accepted for print October 21, 2015*